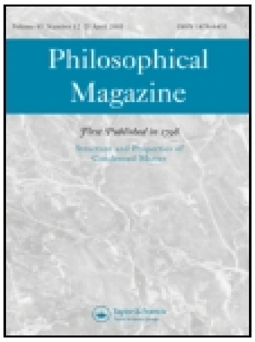

Philosophical Magazine

ISSN: 1478-6435 (Print) 1478-6443 (Online) Journal homepage: https://www.tandfonline.com/loi/tphm20

Partial recrystallization in the nugget zone of friction stir welded dual-phase Cu–Zn alloy

G.M. Xie , Z.Y. Ma & L. Geng

Philosophical Magazine
Vol. 89, No. 18, 21 June 2009, 1505–1516

Taylor & Francis
Taylor & Francis Group

Partial recrystallization in the nugget zone of friction stir welded dual-phase Cu–Zn alloy

G.M. Xie[a,b], Z.Y. Ma[a]* and L. Geng[c]

[a]Shenyang National Laboratory for Materials Science, Institute of Metal Research, Chinese Academy of Sciences, Shenyang 110016, China; [b]State Key Laboratory of Rolling and Automation, Northeastern University, Shenyang 110004, China; [c]School of Materials Science and Engineering, Harbin Institute of Technology, Harbin 150001, China

(*Received 6 November 2008; final version received 2 May 2009*)

For single and quasi-single phase metallic materials, complete dynamic recrystallization has been observed in the nugget zones (NZs) of friction stir welds (FSWs), producing fine and uniform equiaxed grains. In this study, partial dynamic recrystallization was observed in the NZ of 5 mm thick friction stir welded brass plates. Whereas the top and the advancing side of the NZ were characterized by fine completely-recrystallized grains, the remaining region consisted of coarse non-recrystallized deformed grains, annealed recrystallized grains and deformed recrystallized grains. The occurrence of partial recrystallization was attributed to the inhibiting effect of a high volume fraction of fine β'-phase particles. Increasing the FSW passes reduced the fraction and size of non-recrystallized deformed grains, but could not eliminate the partially recrystallized zone completely.

Keywords: friction stir welding; copper alloy; recrystallization; electron backscatter diffraction

1. Introduction

Friction stir welding (FSW) was invented by The Welding Institute of the UK in 1991 as a new solid-state joining technique [1]. During the FSW process, the material undergoes intense plastic deformation and thermal exposure, resulting in the generation of fine and equiaxed recrystallized grains [2]. Welding parameters, tool geometry, material type and work piece thickness have a significant effect on the material flow pattern and temperature field distribution, thereby influencing the microstructural evolution.

Whereas most FSW research efforts have been focused on single-phase or quasi-single phase materials, FSW investigations into the dual-phase materials are limited. For the single phase materials (pure copper) and the quasi-single phase materials (aluminum and magnesium alloys), a complete dynamic recrystallization occurred in the nugget zone (NZ), producing fine and uniform equiaxed grains [3–5]. The existence of two phases in the dual-phase materials would complicate the plastic flow and recrystallization process during FSW. Dual-phase brass (Cu–Zn alloy) with

*Corresponding author. Email: zyma@imr.ac.cn

ISSN 1478–6435 print/ISSN 1478–6443 online

DOI: 10.1080/14786430903019040
http://www.informaworld.com

a higher plasticity, strength, hardness and corrosion resistance than pure copper is a widely used dual-phase copper alloy consisting of α-phase (copper solution) and β'-phase (CuZn compound). Compared to the α-phase, the β'-phase has poor deformation ability and higher hardness. Thus, the flow and recrystallization of brass during FSW might be different from single-phase or quasi-single phase materials due to the existence of a high volume fraction of brittle and hard β'-phase.

Park et al. [6] reported successful FSW of 2 mm thick 60%Cu–40%Zn (hereafter denoted by 60/40 brass) dual-phase alloy sheets under a wide range of FSW parameters with a homogeneous recrystallized structure being observed in the NZ. Subsequently, Meran [7] studied the joint properties of 3 mm thick friction stir welded 70/30 brass plates. From optical micrographs, it appeared that the base material consisted of two phases, athough the 70/30 brass should be a single-phase alloy under equilibrium conditions. However, no description of the as-received microstructure and the microstructural evolution during FSW was given. Very recently, Cam et al. [8] investigated the effect of FSW parameters on the tensile properties of 3 mm thick friction stir welded 90/10 and 70/30 brass plates. However, no information on the microstructure was presented.

In previous work, the present authors reported that partial recrystallization was observed in the NZ of 5 mm thick friction stir welded 62/38 brass plates produced at a wide range of welding parameters [9]. By increasing the rotation rate from 400 to 1000 rpm for a constant traverse speed of 100 mm min^{-1}, the fraction of the non-recrystallized grains decreased. However, even at a higher rotation rate of 1000 rpm, partial recrystallization still existed. This indicates that the increased heat input and enhanced plastic deformation could not eliminate the partial recrystallization. In this study, the microstructure of the partially recrystallized regions was subjected to detailed electron backscatter diffraction (EBSD) examination. Furthermore, additional FSW passes were applied to the original weld to examine the effect of multiple-pass FSW on the partial recrystallization. The aim is to understand the origin of the partial recrystallization in the friction stir welded dual-phase brass.

2. Experimental

5 mm thick commercial brass plates under 1/2H (half of hardness of cold worked brass) condition were used in this study. The nominal chemical composition was Cu–38Zn–0.15Fe –0.08Pb–0.5Ni (wt%). Plates 300 mm in length and 70 mm in width were welded at a tool rotation rate of 600 rpm and a traverse speed of 100 mm min^{-1} along the rolling direction using a gantry FSW machine. A tool with a shoulder 18 mm in diameter and a cylindrical threaded pin 6 mm in diameter and 4.7 mm in length was used. The tilt angle was maintained at 2.5° and the plunged depth was controlled at ~0.2 mm. After the welding was completed, some of the welds were subjected to additional two-pass FSW along the original weld under the same FSW conditions.

The FSW samples were cross-sectioned perpendicular to the welding direction, polished and then etched with a solution of 100 ml distilled water, 15 ml hydrochloric acid and 2.5 g iron(III) chloride. Microstructural features were analyzed by optical microscopy (OM) and an EBSD system (HKL, Channel 4 type). The fraction of the

β'-phase in the parent materials (PM) and the NZ was estimated on the OM micrographs by Scion software.

3. Results and discussion

A defect-free weld was obtained at a rotation rate of 600 rpm and a traverse speed of 100 mm min^{-1}, as shown in Figure 1. Three microstructural zones were identified, i.e. NZ, thermo-mechanically affected zone (TMAZ) and heat affected zone (HAZ). It is noted that the width of the NZ is much larger than that of the pin. However, for aluminum and magnesium alloys and pure copper, the widths of their NZs are only slightly larger than those of the pins [3–5]. This difference is attributed to the lower stacking fault energy (SFE) for α-phase in brass (3.5×10^{-2} J m^{-2}) compared to pure copper (7×10^{-2} J m^{-2}), aluminum (20×10^{-2} J m^{-2}) and magnesium (8×10^{-2} J m^{-2}) [10]. It is well documented that a low SFE tends to suppress recovery and promote recrystallization. Therefore, under the stirring effect of the rotating tool, dynamic recrystallization (DRX) occurred in a larger region in brass than in aluminum and magnesium alloys and pure copper, thereby producing a wider NZ in brass.

Compared to the homogeneous NZs in 2 mm thick friction stir welded brass sheets [6], an inhomogeneous NZ was observed in the present 5 mm thick friction stir welded brass plates, as shown in Figure 1. The inhomogeneous NZ could be divided into three sub-zones, i.e. NZ1, NZ2 and NZ3. NZ2 and NZ3 appeared in the top side and advancing side of the NZ, respectively. Similarly, Ma et al. [11] reported that for friction stir processed (FSP) A356 alloy, an obvious banded structure was observed in the advancing side of the NZ for some parameter combinations. Furthermore, Schneider and Nunes [12] noted that for friction stir welded Al–Li–Cu alloy, visible "onion rings" were found in the advancing side of the NZ. This indicates that inhomogeneous plastic deformation appeared in the NZ under some conditions.

Figure 2 shows the microstructures of the PM, NZ1, NZ2 and NZ3, respectively. The PM was characterized by coarse α-phase and β'-phase in between with the smooth grain boundaries and a number of twins in the α-phase (Figure 2a). The fraction of the β'-phase in the as-received 62/38 brass was estimated to be 27%, which is substantially higher than that (~16%) in the 60/40 brass as reported by Park et al. [6]. According to the binary phase diagram of the Cu–Zn alloy (Figure 3), 62/38 brass should contain a lower fraction of the β'-phase, compared to the 60/40 brass, under an equilibrium condition. The higher fraction of the β'-phase indicates that the as-received 62/38 brass plate was prepared under a non-equilibrium condition. The NZ1 was characterized by coarse strip-like non-recrystallized grains

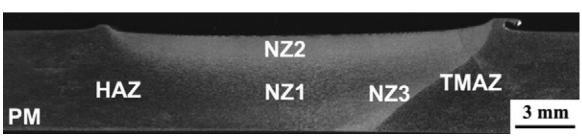

Figure 1. Cross-sectional macrograph of friction stir welded 62/38 brass joint (the advancing side is on the right).

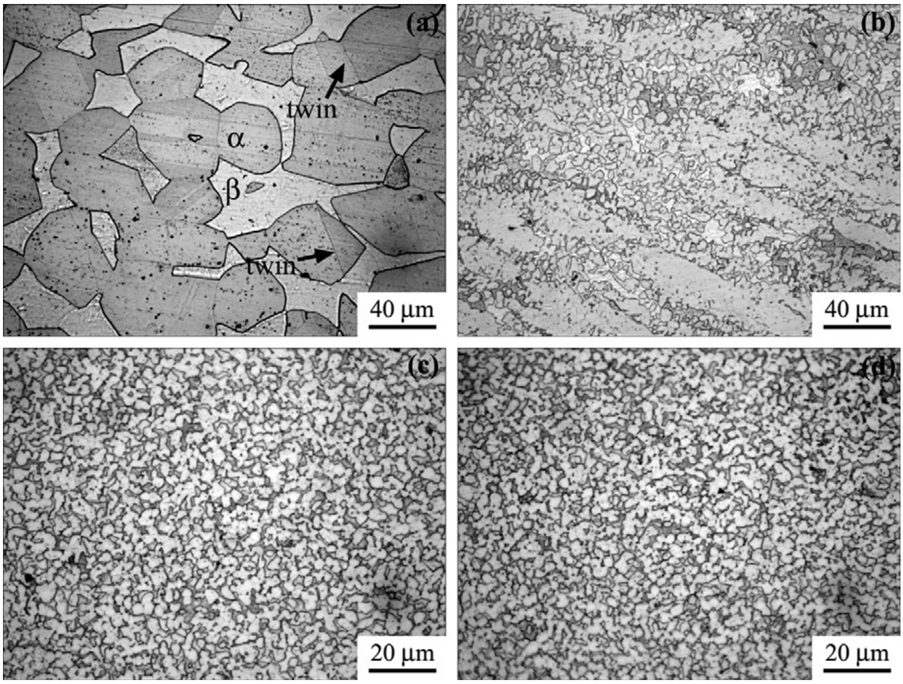

Figure 2. Optical micrographs of friction stir welded 62/38 brass joint: (a) PM; (b) NZ1; (c) NZ2; (d) NZ3.

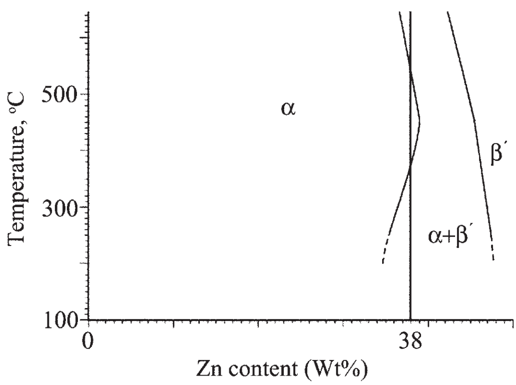

Figure 3. Local binary phase diagram of Cu–Zn alloy [13].

and fine recrystallized grains (Figure 2b). The reason for the formation of the non-recrystallized deformed grains will be further discussed later. Compared to the NZ1, both NZ2 and NZ3 consisted of finer completely-recrystallized grains and exhibited similar microstructural characteristics (Figures 2c and 2d). This is attributed to more intense plastic deformation experienced in the NZ2 that contacted the shoulder and in the NZ3 where the shearing rate was higher than that at the retreating side.

Figure 4a presents the grain orientation map in the NZ1. The black and white lines represent the high angle grain boundaries (HAGBs, grain boundary orientation angle $>15^\circ$) and low angle grain boundaries (LAGBs, grain boundary orientation angle $<15^\circ$), respectively. The number fraction of the HAGBs was determined to be 83.6% in the NZ1 and the grain boundary misorientation angle for the highest frequency appeared at $\sim 60^\circ$ (Figure 4b). Figure 4c shows the distribution of the $\Sigma 3$ grain boundaries with the boundary misorientation angles of $60 \pm 5^\circ$, measured by EBSD. The $\Sigma 3$ grain boundaries made up 31% of all the boundaries. These $\Sigma 3$ grain boundaries are universally considered as the coherent annealing twin grain boundaries at $\langle 111 \rangle$ plane, and also known as coincidence site lattice (CSL) grain boundaries [14]. The CSL grain boundaries play an important role in improving the resistance to brittle cracking and intergranular corrosion [14]. Oh-ishi et al. [15] reported that for FSP Ni–Al bronze, the number fractions of the HAGBs in the central zone of the NZ were higher than 90%. Furthermore, Oh-ishi et al. [15] also noted that the NZ of the FSP bronze contained a large number of the $\Sigma 3$ twin grain boundaries. Clearly, the number fraction of the HAGBs in the NZ1 of the present friction stir welded brass is lower than that in the NZ of the friction stir processed bronze. This is attributed to the appearance of non-recrystallized deformed grains with a great number of subgrains.

For hot deformed metals, the magnitude of the internal average misorientation angle (IAMA) of subgrains in the grains represents the magnitude of the stored energy in the grains. With an increasing IAMA, the stored energy of the grains gradually increases. Therefore, the grains in the hot deformed materials can be divided into three types, i.e. low stored energy (LSE) grains ($\mathrm{IAMA} < 2^\circ$), middle stored energy (MSE) grains ($2^\circ < \mathrm{IAMA} < 7.5^\circ$), and high stored energy (HSE) grains ($7.5^\circ < \mathrm{IAMA} < 15^\circ$). Figures 5a and 5b show the distribution and frequency of the LSE zone (blue zone), the MSE zone (yellow zone) and the HSE zone (red zone). The coarse non-recrystallized grains in Figure 4a correspond to the red zone in Figure 5a and the ratio of the HSE grains was relatively high (Figure 5b). Therefore, during FSW, a number of coarse grains in the PM underwent intense plastic deformation, but did not recrystallize. The fine recrystallized grains in Figure 4a are consistent with the blue and yellow zones in Figure 5a. The grains with the annealing twin boundaries in Figure 4c coincided with the blue region in Figure 5a, indicating that the LSE grains were annealed recrystallized grains. During FSW, parts of the recrystallized grains were deformed, thereby resulting in the appearance of recrystallized grains with a MSE (yellow zone). Therefore, the recrystallized grains included the annealed recrystallized grains and deformed recrystallized grains. Based on the above observations, it can be concluded that the NZ1 consisted of coarse non-recrystallized deformed grains, annealed recrystallized grains and deformed recrystallized grains. The EBSD results are in good agreement with OM observations (Figure 2).

In the past few years, extensive studies showed that complete dynamic recrystallization occurred in the NZs of friction stir welded aluminum and magnesium alloys and pure copper [3–5], thereby producing the NZs with the relatively homogeneous recrystallized grains. Clearly, the present observations of the 5 mm thick friction stir welded brass plates differ from those of the friction stir welded aluminum and magnesium alloys and pure copper, and even from those of 2 mm

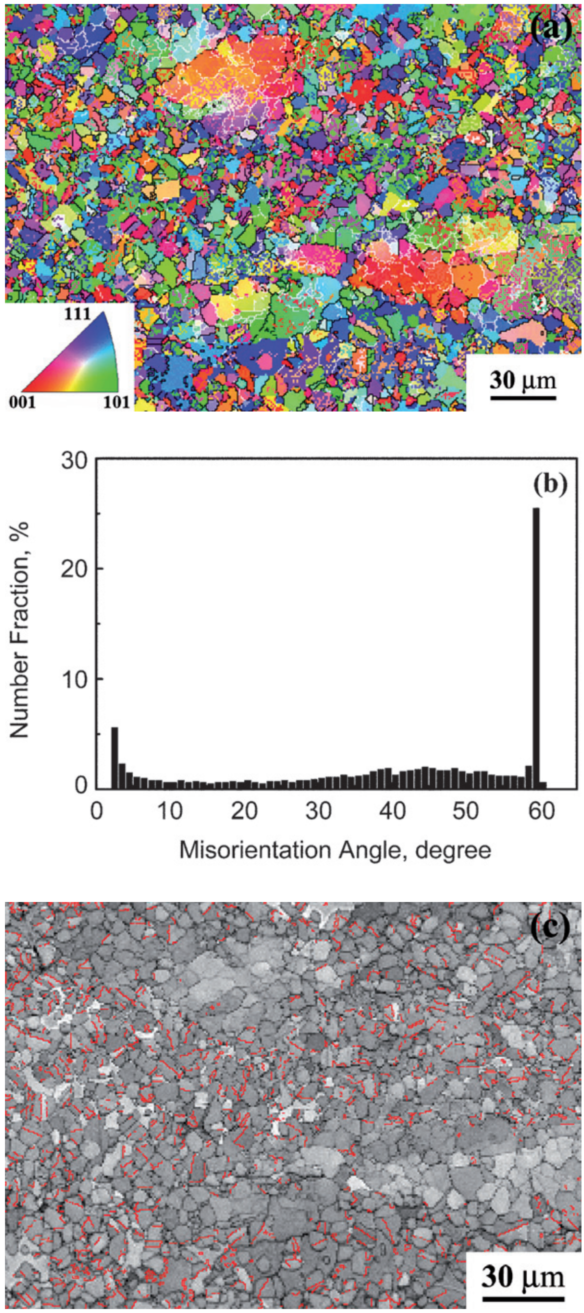

Figure 4. (a) Distributions of misorientation, (b) distribution of grain boundary misorientation angle and (c) distribution of Σ3 twin grain boundaries (red lines) in the NZ1 of friction stir welded 62/38 brass joint.

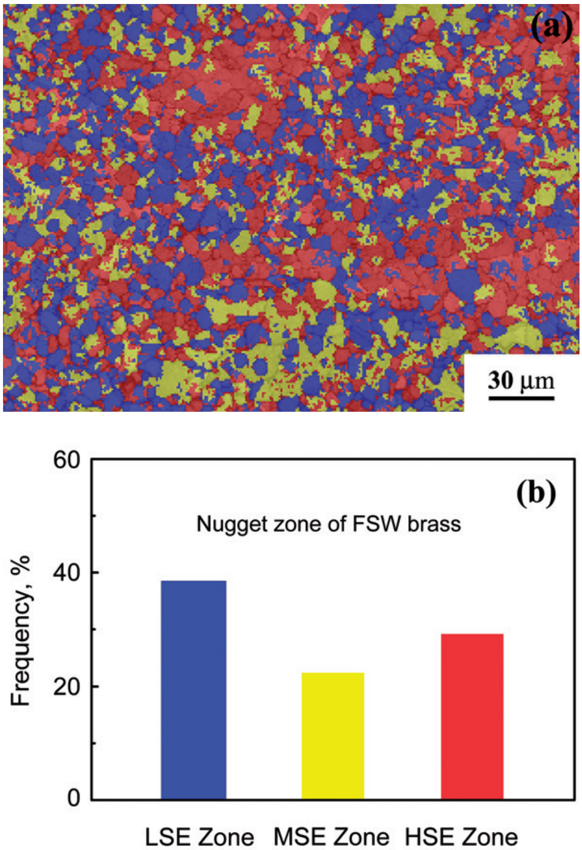

Figure 5. (a) Distribution map and (b) frequency of low stored energy (LSE), middle stored energy (MSE) and high stored energy (HSE) zones in the NZ1 of friction stir welded 62/38 brass joint.

thick friction stir welded brass sheets [6]. As discussed above, the lower SFE of the α-phase in brass would promote the occurrence of recrystallization. Therefore, the partial recrystallization observed in the present 5 mm thick friction stir welded brass plate is surprising. This might be attributed to the following reasons. First, high thermal conductibility and thicker dimension of the brass plate used in this study made it hard to achieve a homogeneous plastic flow throughout the whole NZ due to the gradients in strain, strain rate and temperature [16]. Second, a high volume fraction of fine β'-phase particles, mainly distributed in the coarse non-recrytallized deformed grains, as shown in Figure 6, might inhibit the plastic flow and the recrystallization process of the α-phase.

It is well documented that particles play an important role in the recrystallization process by particle-stimulated nucleation (PSN). Humphreys and Kalu [17] and McNelley et al. [16] noted that the size of non-deforming particles influenced recrystallization by PSN in an alloy. When the non-deforming particles were bulky, highly misoriented cells or subgrains formed in the zones surrounding the particles, promoting recrystallization. On the contrary, fine non-deforming particles could

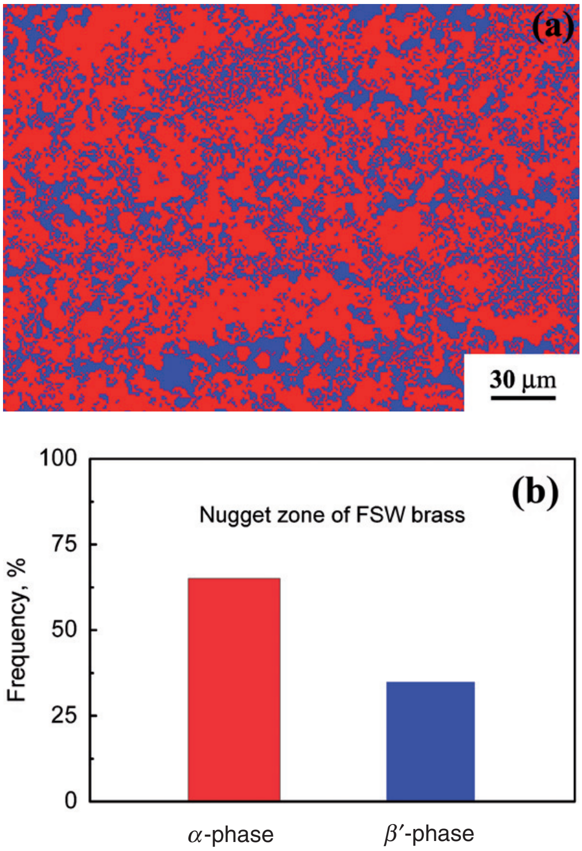

Figure 6. (a) Distribution and (b) frequency of α-phase (red) and β'-phase (blue) in NZ1 of friction stir welded 62/38 brass joint.

inhibit recrystallization. For the present friction stir welded 62/38 brass, a high fraction of the β'-phase particles, which were of various sizes, indicated that the situation for PSN in the friction stir welded dual-phase brass is quite different from that in quasi-single phase materials with only limited volume fraction of the particles.

The fraction number of the β'-phase in the NZ was determined to be 34.9%, higher than that in the as-received brass (27%). Previously, Park et al. [6] also reported an increase in the fraction of the β'-phase in the NZ compared to the PM. This indicated that part of the α-phase was transformed to β'-phase during FSW. The transformed β'-phase remained in the NZ after FSW due to fast cooling from FSW temperatures. Figures 4a and 6 clearly indicate that the coarse non-recrystallized grains contained a high density of the fine β'-phase particles. In this case, dynamic recrystallization was prohibited in some regions of the NZ in 5 mm thick friction stir welded brass due to an insufficient plastic deformation and the pinning of the fine β'-phase particles. For single phase or quasi-single phase

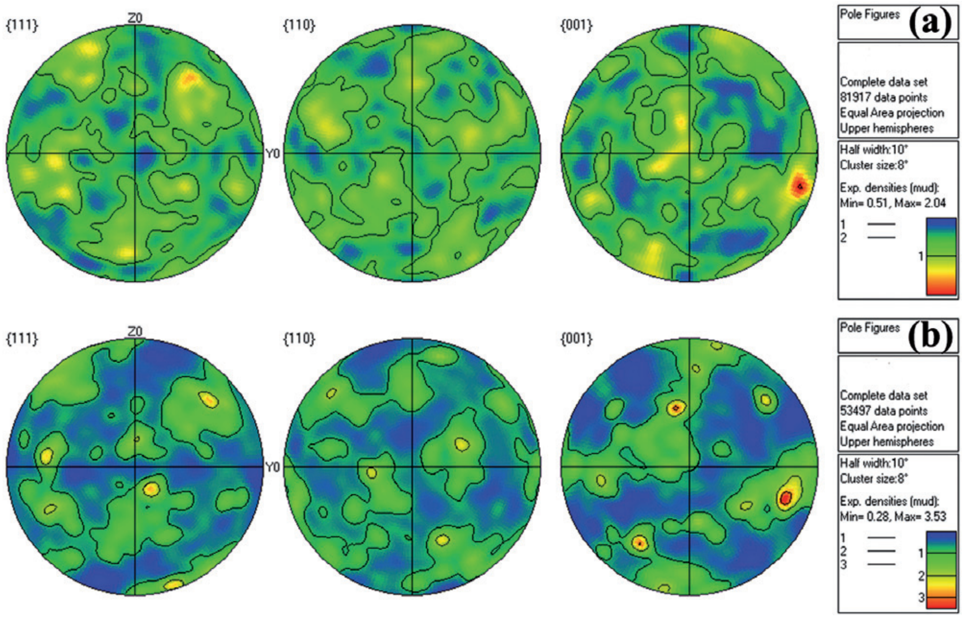

Figure 7. (Color online). Pole figures of (a) α and (b) β' phases for NZ1 in friction stir welded 62/38 brass joint.

materials, such as aluminum alloys, magnesium alloys, and pure copper, inhomogeneous plastic deformation could result in the occurrence of "onion ring" or banded structure. However, dynamic recrystallization would not be impeded due to the absence or limited number of second phase particles [3–5]. In some situations, recrystallization would be promoted by PSN [16,17].

Recently, most investigations of the texture of friction stir welds have been focused on magnesium and aluminum alloys [18–21], whereas reports on copper alloys are quite limited [15]. Figure 7 shows the pole figures of α and β' phases in the NZ1. As indicated, the NZ1 exhibits a relatively random texture. This is attributed to the occurrence of the dynamic recrystallization that destroyed the original texture of the PM. Similarly, Oh-ishi et al. [15] reported that the random α-phase texture was observed throughout the NZ of the FSP bronze.

In order to investigate the effect of plastic deformation on the recrystallization in the friction stir welded brass, two additional FSW passes were applied to the original weld under the same FSW conditions. It is indicated that increasing the FSW pass, i.e. plastic deformation, resulted in an increase in the completely recrystallized zones (NZ2 and NZ3) (Figure 8). However, the partial recrystallized zone (NZ1) was not completely eliminated. Furthermore, the size and fraction of the non-recrystallized deformed grains in the NZ1 were significantly lower than those in the one-pass friction stir welded sample (Figures 9a and 2b). In the completely recrystallized zones (NZ2 and NZ3), the grain size achieved by three-pass FSW was similar to that by one-pass FSW (Figures 2c–2d and 9b–9c).

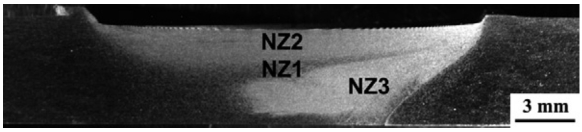

Figure 8. Cross-sectional macrograph of friction stir welded 62/38 brass joint with three FSW passes (the advancing side is on the right).

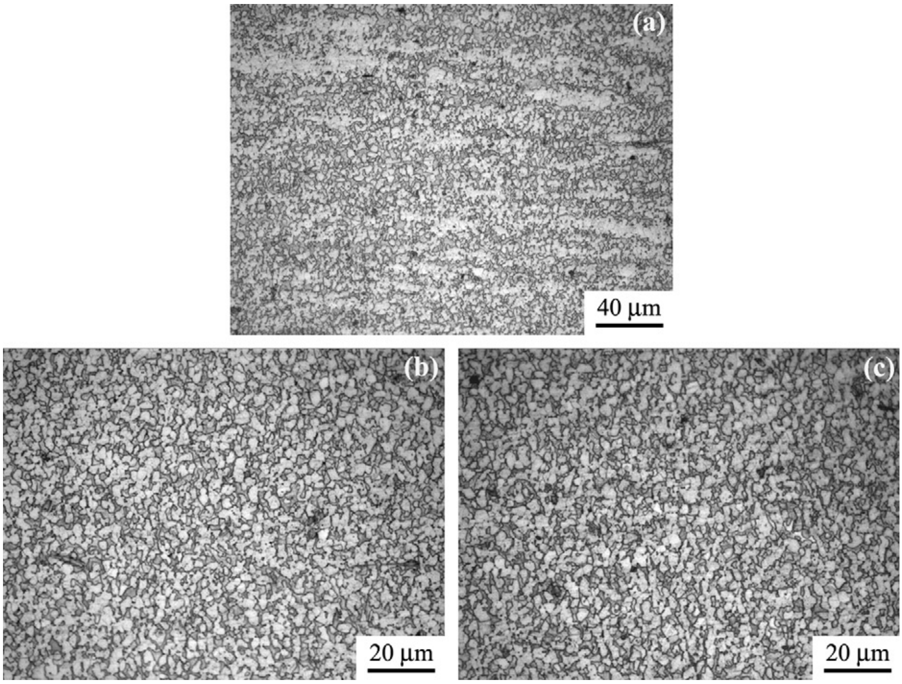

Figure 9. Optical micrographs of friction stir welded 62/38 brass joint with three FSW passes: (a) NZ1; (b) NZ2; (c) NZ3.

In a previous study [9], it was indicated that increasing the tool rotation rate resulted in a decrease in the fraction of the partially recrystallized zone. However, even at a high heat input condition of 1000 rpm, the partial recrystallization could not be completely eliminated. Therefore, the partial recrystallization in the thick FSW brass plate was mainly attributed to the existence of a high volume fraction of the β'-phase. Increasing the heat input and plastic deformation amount increased the fraction of the recrystallized zone, but could not eliminate the partially recrystallized zone, due to the inhibition of a large number of β'-phase particles in the recrystallization. However, the partially recrystallized zone in the NZ did not affect the mechanical properties of 5 mm thick friction stir welded 62/38 brass joints because the fracture of the joints occurred at the HAZ, not the NZ [9]. The HAZ was the softest zone and the NZ had higher hardness due to significant grain refinement [9].

4. Conclusion

(1) FSW resulted in significant refinement in both α and β'-phase grains in 5 mm thick friction stir welded 68/32 dual-phase brass plate. Furthermore, part of the α-phase was transformed to the β'-phase during FSW, resulting in an increase in the fraction of the β'-phase in the NZ.

(2) Whereas the top and the advancing side of the NZ were characterized by fine completely-recrystallized grains, partial dynamic recrystallization was observed in the remaining region.

(3) The partially recrystallized zone was characterized by a high ratio of the HAGBs (83.6%) and a relatively random texture, and consisted of coarse non-recrystallized deformed grains with high stored energy, fine deformed recrystallized grains with middle stored energy and annealed recrystallized grains with low stored energy.

(4) The existence of a high volume fraction of the β'-phase in the 68/32 brass resulted in heterogonous plastic deformation during FSW and inhibited the dynamic recrystallization, thereby producing the partial recrystallization.

(5) Increasing the FSW passes, i.e. plastic deformation, could not eliminate the partially recrystallized zone.

Acknowledgements

This work was supported by the National Outstanding Young Scientist Foundation under Grant No. 50525103, the National Basic Research Program of China under Grant No. 2006CB605205, and the Hundred Talents Program of Chinese Academy of Sciences.

References

[1] W.M. Thomas, E.D. Nicholas, J.C. Needham, M.G. Murch, P. Templesmith and C.J. Dawes, GB Patent Application No. 9125978.8, December 1991.
[2] R.S. Mishra and Z.Y. Ma, Mater. Sci. Eng. R 50 (2005) p.1.
[3] G.M. Xie, Z.Y. Ma and L. Geng, Scripta Mater. 57 (2007) p.73.
[4] K.V. Jata and S.L., Semiatin, Scripta Mater. 43 (2000) p.743.
[5] G.M. Xie, Z.Y. Ma, L. Geng and R.S. Chen, Mater. Sci. Eng. A 471 (2007) p.63.
[6] H.S. Park, T. Kimura, T. Murakami, Y. Nagano, K. Nakata and M. Ushio, Mater. Sci. Eng. A 371 (2004) p.160.
[7] C. Meran, Mater. Des. 27 (2006) p.719.
[8] G. Cam, H.T. Serindag, A. Cakan, S. Mistikoglu and H. Yavuz, Materialwiss. Werkst. 39 (2008) p.394.
[9] G.M. Xie, Z.Y. Ma and L. Geng, Mater. Trans. 49 (2008) p.1698.
[10] R.Z. Tang, *Physical Metallurgy Basics*, China Metallurgy Industry Press, Beijing, 1997, p.8.
[11] Z.Y. Ma, S.R. Sharma and R.S. Mishra, Mater. Sci. Eng. A 433 (2006) p.269.
[12] J.A. Schneider and A.C. Nunes, Metall. Mater. Trans. B 35 (2004) p.777.
[13] E. Hornbogen, Z. Metallkd. 50 (1959) p.70.
[14] H. Davies and V. Randle, J. Microsc. 205 (2002) p.253.
[15] K. Oh-ishi, A.P. Zhilyaev and T.R. McNelley, Metall. Mater. Trans. A 37 (2006) p.2239.
[16] T.R. McNelley, S. Swaminathan and J.Q. Su, Scripta Mater. 58 (2008) p.349.

[17] F.J. Humphreys and P.N. Kalu, Acta Metall. Mater. 35 (1987) p.2815.
[18] R.W. Fonda and J.F. Bingert, Scripta Mater. 57 (2007) p.1052.
[19] W. Woo, H. Choo, D.W. Brown, S.C. Vogel, P.K. Liaw and Z. Feng, Acta Mater. 54 (2006) p.3871.
[20] Y.S. Sato, H. Kokawa, K. Ikeda, M. Enomoto, S. Jogan and T. Hashimoto, Metall. Mater. Trans. A 32 (2001) p.941.
[21] S.H.C. Park, Y.S. Sato and H. Kokawa, Metall. Mater. Trans. A 34 (2003) p.987.